

Linear-drifting subpulse sources in radio pulsars

P. B. Jones*

*University of Oxford, Department of Physics, Denys Wilkinson Building,
Keble Road, Oxford OX1 3RH, U.K.*

ABSTRACT

Analysis of plasma acceleration in pulsars with positive corotational charge density has shown that any element of area on the polar cap is bi-stable: it can be in phases either of pure proton emission or of mixed ions and protons (the ion phase). Ion-phase zones are concentrated near the edge of the polar cap, and are a physical basis for the coherent radio emission observed as components within the mean pulse profile. The state of the polar cap is generally chaotic, but organized linear motion of ion zones in a peripheral band is possible and is the likely source of sub-pulse drift. It is shown that several patterns of limited movement are possible and can account for the varied phenomena observed including mirror and bi-directional drifting.

Key words: instabilities - plasma - stars: neutron - pulsars: general

1 INTRODUCTION

The phenomenon of subpulse drift in radio pulsars has been observed extensively for more than four decades. The most complete published survey, that of Weltevrede, Edwards & Stappers (2006), found it to be present in about one half of a sample of 187 pulsars, selected only by signal-to-noise ratio. Usually, subpulses within a window defined by the averaged pulse profile are observed to drift in successive periods to either more negative or positive longitudes. But extremely complex behaviour has been seen in some individual pulsars. The direction of drift can change from negative to positive, or vice-versa. Bi-directional drifting, in which two or more subpulses within the window of observation simultaneously drift in opposite directions, has been seen in a small number of multi-component pulsars, specifically in B1839-04 (Weltevrede et al 2006) and in J0815+09 (Champion et al 2005). Very irregular patterns of drift are seen in the multi-component B0826-34 in which the rates change sign smoothly over sequences of the order of 10 periods in length (Gupta et al 2004). There are many other cases of complex behaviour such as B0818-41 (Bhattacharyya et al 2007, Bhattacharyya, Gupta & Gil 2009). Also, it is thought likely that the close association of subpulse drift with mode-changes and nulls, for example in B1918+19 (Rankin, Wright & Brown 2013) will be an important diagnostic of polar-cap physics and radio-emission, particularly in pulsars within the age range 1 – 10 Myr.

Very many authors have sought to describe subpulse motion in terms of the classic model introduced by Ruderman & Sutherland (1975) in which localized regions

of electron-positron pair production, referred to as sparks, move in a circular $\mathbf{E} \times \mathbf{B}$ drift around the polar cap. There has been some limited development of this by Deshpande & Rankin (1999), van Leeuwen & Timokhin (2012), also by Gil, Melikidze & Geppert (2003) who assumed the existence of a temperature-dependent ion component in the pair plasma. Although the basis of the model is an electric-field boundary condition $\mathbf{E}_{\parallel} \neq 0$ at the polar-cap surface, it is widely used phenomenologically with no reference to boundary conditions. (The subscripts \parallel and \perp refer to directions locally parallel with and perpendicular to the magnetic flux density \mathbf{B} .) Also neglected is the sign of $\boldsymbol{\Omega} \cdot \mathbf{B}$ at the polar cap, where $\boldsymbol{\Omega}$ is the rotation spin.

In this paper, and based on cohesive energy calculations (see Jones 1985, Medin & Lai 2006), it is assumed that the $\mathbf{E}_{\parallel} \neq 0$ boundary condition is not satisfied except possibly in the extremely small fraction of pulsars known to have polar-cap dipole fields of the order of $B \sim 10^{14}$ G. But spin-down rates measure only the dipole moment and we have to bear in mind that actual polar magnetic flux densities could be significantly increased in the presence of higher multipoles. Thus recent numerical modelling of internal field evolution (Geppert, Gil & Melikidze 2013) has shown that Hall drift, given suitable initial conditions, can lead to the formation of small-area magnetic anomalies, close to the magnetic pole, with the required values of B . Geppert et al, who also comprehensively survey earlier work on Hall drift, discuss the likelihood that these initial conditions are valid. The most significant is the existence of a strong ($\sim 10^{15}$ G) internal toroidal field component within the crust which must extend to regions close to the poles. In an axisymmetric example of these authors' calculations, Hall drift amplifies an initial 10^{13} G dipole field by almost an order of magnitude

* E-mail:p.jones1@physics.ox.ac.uk

in 10^6 yr; it also promotes pair creation by decreasing the flux-line radius of curvature by between one and two orders of magnitude. But we return to this question in Section 5.

Comparisons of the model with observational results have been published for many pulsars. A list, which is not complete, includes B0943+10 (Deshpande & Rankin 2001), B0818-13 (Janssen & van Leeuwen 2004), B1857-26 (Mitra & Rankin 2008), J1819+1305 (Rankin & Wright 2008), B1133+16 (Honnappa et al 2012). In certain cases, the presence of some evidence for periodicity has led to the estimation of a carousel circulation time $\hat{P}_3 = nP_3$ in the usual notation, where n is here the number of sparks or subpulses and P_3 is the observed time interval between the appearance of successive subpulses at a given longitude. The model predicts a unique direction of $\mathbf{E} \times \mathbf{B}$ drift so that the observed cases of bi-directional sub-pulse drift are assumed to arise from the presence of aliasing, a change from one Nyquist zone to the adjacent. A positive feature of the model is that the field \mathbf{E} and hence the drift velocity can be estimated. However, the complexity and heterogeneity of subpulse drift and of nulls and mode-changes is perhaps an indication that physics beyond that of electromagnetic fields and boundary conditions is involved.

In previous work, we have shown that in the $\boldsymbol{\Omega} \cdot \mathbf{B} < 0$ case, and with the space-charge-limited flow boundary condition, the blackbody radiation field of the neutron star interacting with accelerated ions creates a reverse electron flux incident on the polar cap. The electromagnetic showers formed are a source of protons through the decay of the giant dipole state and their estimated diffusion time to the surface is of the order of a typical neutron-star rotation period. It was shown that zones of ion and proton emission are a physical basis for subpulse formation and radio-frequency emission through the growth of a two-beam instability.

An important question is whether or not there is any observational evidence for the existence of an accelerated ion-proton plasma. Recent operation of LOFAR by Hassall et al (2012) has placed severe constraints on the size and altitude of the 40 MHz emission from several pulsars and from PSR B1133+16 in particular. On the basis of these results, it has been argued elsewhere (Jones 2013a) that an electron-positron plasma cannot be the source of emission in this pulsar.

We refer to Jones (2013b) and earlier papers cited therein for further details of the model. In this paper, Section 2 gives a brief summary of the properties of the ion and proton zones on the polar cap.

The reverse electron flux has the same effect as pair creation in limiting the potential difference available for ion and proton acceleration. Thus the outward moving plasma consists of relativistic, but not ultra-relativistic, ions and protons with negligible pair creation. The loss of acceleration field \mathbf{E}_\parallel limits the area of the active polar cap in the way described by Arons & Scharlemann (1979). Unfavourably curved magnetic flux lines from the inactive sector, as defined by Arons & Scharlemann, form a dead volume in the open magnetosphere of pulsars that are unable to support pair creation. It is not unreasonable to assume, as in this paper, that the magnetic flux lines in the region of radio emission are simply those of a dipole. But the real problem is that the shape of the active polar cap is determined by the field distribution near the light cylinder which is not well

understood, particularly in the absence of pair creation (see Muslimov & Harding 2004, 2009).

The loss of polar-cap symmetry through the presence of the dead volume and the results of further running of the polar-cap model described in Jones (2013b) both suggest that the carousel model is not actually realized. There is, of course, no observational evidence that demands subpulse motion on a closed curve; only evidence of drift within the band of flux lines that are observable. Given our physical model for subpulse formation, it is possible to envisage much more simple systems of drift that are able to produce quite naturally the complex forms of behaviour described above. The computational results from the model are described in Section 3 and the proposed form of drifting in Section 4. Our conclusions are given in Section 5.

2 BASIS OF THE SUBPULSE MODEL

A summary of the properties of our model can start with proton formation in the electromagnetic showers produced by the reverse photo-electron flux. A Green function describes proton diffusion from the point of formation at the shower maximum to the upper extremity of the ion atmosphere which we assume to exist in local thermodynamic equilibrium (LTE) at the polar-cap surface. The structure of the atmosphere is defined by the ions which are more numerous than the protons. The protons are never in static equilibrium and a small electric field present within the charge-neutral atmosphere drives them through to its upper extremity. Thus we adopt a δ -function approximation for the Green function so that a shower formed at time t produces protons at $t + \tau_p$ at the base of the acceleration region. It has been estimated that τ_p is of the order of one second which is a typical pulsar period P . Protons at the top of the atmosphere are preferentially accelerated. If the rate of proton production exceeds the Goldreich-Julian flux, ρ_{GJC}/e , the excess protons form a layer with number density n_p at the top of the LTE ion atmosphere and acceleration of ions ceases. With our simple Green function, this occurs at a time τ_p after the start of ion acceleration.

It has to be emphasized that the process described above is quite local. It must be true that both accelerated ions and reverse electrons experience $\mathbf{E} \times \mathbf{B}$ drift but, because the time constant τ_p is many orders of magnitude longer than particle transit times, it has negligible effect on the evolution of the system. Any element of area on the active polar cap is either in a proton zone or an ion zone according to the character of the accelerated plasma. Our Green function is a useful but by no means accurate approximation so that the ion zone will, in general, have both proton and ion components. This, of course, is necessary if the two-beam instability is to exist and result in coherent radio emission. We refer to Buschauer & Benford (1977) for the relativistic Penrose condition which, in the general case, governs its growth rate. But proton zones have only a single component because there is an accumulation of protons at the top of the LTE atmosphere and there is no possibility of their contributing to coherent emission.

In the model, the number of protons formed per unit area in an ion zone of duration τ_p is sufficient to support a proton zone of duration $\tilde{K}\tau_p$ at the coordinates \mathbf{u} of a point

on the active polar cap, \tilde{K} being a function primarily of the surface nuclear charge Z_s at \mathbf{u} , the acceleration potential difference existing on flux lines leaving the surface at \mathbf{u} , and of the neutron-star blackbody temperature T_s averaged over a fairly large surface area, extending beyond the open polar cap and subtending possibly as much as a steradian.

Successive values of \tilde{K} at a given point therefore fluctuate within a large interval. The shape and disposition of ion zones is chaotic but not random. From a given initial state the condition of an element of area at \mathbf{u} on the polar cap at some future time depends on the sequence of previous values of \tilde{K} at all points on the polar cap. This in turn depends on the history of the acceleration potential over the entire polar cap. The time constant τ_p is so long compared with particle transit times that the acceleration potential can be obtained from Poisson's equation, with fixed boundary conditions. We emphasize again that these considerations, and not $\mathbf{E} \times \mathbf{B}$ drift, determine the shape-change and movement of an ion zone.

3 MODEL RESULTS AND SUBPULSE DRIFT

A complete description of the way in which computational results have been obtained from the model polar cap is contained in Jones (2013b). However, we shall summarize here those features that are of immediate interest.

The polar cap is assumed circular and initially divided into $n_s = N^2$ elements of equal area arranged in N concentric annuli, the central element being a circle of radius u_0/N , where u_0 is the polar-cap radius,

$$u_0 = \left(\frac{2\pi R^3}{cP f(1)} \right)^{1/2}. \quad (1)$$

In this, P is the rotation period, $R = 1.2 \times 10^6$ cm is the neutron-star radius and $f(1) = 1.368$ for a $1.4 M_\odot$ star (Muslimov & Harding 2001). The polar-cap magnetic flux density is 3×10^{12} G and the selected periods $P = 1, 2, 3$ s.

In the initial state, all elements are proton zones. Selected in a random sequence, and with randomly chosen time intervals, all elements make the transition to the ion phase. After each transition, self-consistent solutions are obtained for all ion zones (the complete polar cap) giving individually the degree of ionization of the ions, the energy flux of reverse photo-electrons, and the acceleration potential on the cell axis. Each transition back to the proton phase occurs after an interval τ_p at which time the duration $\tilde{K}\tau_p$ of the subsequent proton phase has been calculated. After each transition from an ion to a proton phase there is a further solution for self-consistency of the complete polar cap. The model is elementary in character but has the considerable advantage that each set of calculations made between the transition to the ion phase in a particular element and its reverse at a time τ_p later is self-contained. Thus the program can be allowed to run for as long a time as is convenient without the accumulation of errors.

The more significant results of such runs, for $N = 10$ were the extent of polar-cap potential fluctuations on time-scales of the order of τ_p and that, at any instant, most ion-phase elements are positioned near the boundary at $\mathbf{u} \approx \mathbf{u}_0$. The latter is entirely consistent with the two-component emission structure (described as conical) observed in many

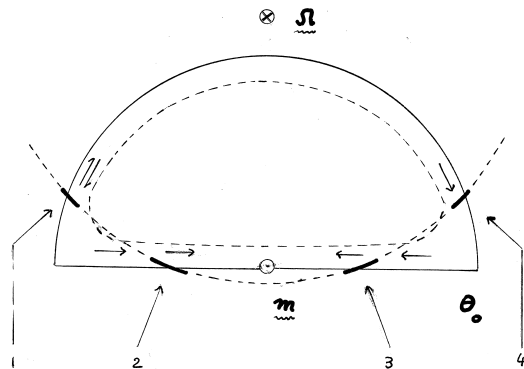


Figure 1. The polar diagram with the magnetic axis \mathbf{m} as origin shows the line of sight, spin Ω , and the tangents to the active open magnetosphere at altitude $\eta = 10$ and polar angle $\theta_0 = 4.6^\circ$. The peripheral band of flux lines supporting emission is shown schematically as a closed broken curve. Relative to the magnetosphere, the line of sight transits on a curve shown by the broken line whose intersections with the peripheral band give four components within the mean pulse profile. Arrows show the directions ion-zone drift that correspond with the observed pattern of B0815+0939. The transit curve is drawn approximately to scale so as to reproduce the 100° mean profile width of this pulsar, and is at an angle of $\sim 6^\circ$ with $-\Omega$. The components seen are labelled 1 – 4 in order of increasing longitude, the first being described as indistinct by Champion et al.

pulsars, and is an anticipated consequence of the variation of the time-averaged value of \tilde{K} as a function of \mathbf{u} . Computation of the autocorrelation function for the azimuthal distribution of ion-zone elements near \mathbf{u}_0 also gave evidence of the preferential formation of small clusters which could be the source of sub-pulses. Although obtained for a circular polar cap, these results are qualitatively independent of polar-cap shape and would remain valid for the approximate form we assume in the following Section.

A modified version of the program with $N = 10$ has the $2N - 1 = 19$ elements of the outer annulus increased to 60 in order to facilitate the search for naturally occurring subpulse drift similar to the carousel model of Ruderman & Sutherland. In a further optional modification, all elements except those in the outer annulus are at all times in the proton phase so that the symmetry of the acceleration potential about the magnetic axis is disturbed only by ion-phase elements in the outer annulus. Even with this unrealistic structure, attempts to see if subpulses formed in the outer annulus with an initial drift settle down to stable and continuous long-term drifting have met with no success. Subpulses prove to be unstable after no more than several complete rotations. In itself, this result is unremarkable and may be no more than a consequence of the limitations of the program. But the significant result is that if elements in the inner annuli are permitted to undergo transitions to and from the ion phase, any stable subpulse structure there is in the outer annulus is destroyed almost immediately.

The presence of chaotic ion-zone regions in the central part of the polar cap is to be expected and cannot be sim-

ply an artefact arising from the limitations of our model and program. Hence it is difficult to see how the degree of stability necessary for long-term carousel motion can exist.

In Section 1, we noted that some authors have been able to find what is interpreted as a carousel rotation time by measurements of P_3 combined with estimates of the integer number of sparks, or by two-dimensional longitude-resolved fluctuation power spectra formed from long sequences of successive pulses (see, for example, Rankin et al 2013). But failing direct observation of the whole polar cap, these can be no more than evidence for a periodicity. The following Section introduces a simple linear drift pattern which is less demanding of long-term stability and appears more able to accommodate the sui generis nature of many pulsars.

4 PATTERNS OF LINEAR DRIFT

Before proceeding to a description of the linear drift patterns, it is necessary to mention briefly those factors that make the generation of coherent radio emission possible. The exponential amplitude growth factor $\exp \Lambda$ for the two-beam instability assumed to be the source is given by,

$$\Lambda \approx 2.4 \times 10^5 \left(\frac{B_{12} m Z_\infty}{PM \gamma_{A,Z}^3} \right)^{1/2} (1 - \eta^{-1/2}) \quad (2)$$

at radius $r = \eta R$. Here B_{12} is the polar-cap magnetic flux density in units of 10^{12} G, m is the electron rest-mass, and Z_∞ is the final charge of the accelerated ion. The ion mass is M , $\gamma_{A,Z}$ is its Lorentz factor, and P is the rotation period in seconds. The exponent Λ is a slowly varying function of the proton fraction of the polar-cap current density which we here assume to be 0.2. We refer to Jones (2012) for the derivation of this expression.

Equation (2) shows that much of the gain in amplitude occurs at altitudes, $\eta < 2$, beyond which some further acceleration through the Lense-Thirring effect (Muslimov & Tsygan 1992) can occur in principle unless blocked by continuing photo-ionization. But the larger part of the gain is at altitudes above those where most of the acceleration occurs. These considerations are significant because, as equation (2) demonstrates, the exponent Λ is dependent on the ion Lorentz factor. Amplitude gains can be very large for ions that are accelerated from regions \mathbf{u} of the polar-cap surface close to the the boundary \mathbf{u}_0 because they experience a small \mathbf{E}_{\parallel} field. Ions of greater Lorentz factor have smaller Λ so that, given the exponential form of the gain, a sharp cut-off would be anticipated at some critical value of $\gamma_{A,Z}$. In general, the model described in Section 3 has a time-averaged acceleration potential difference which as a function of \mathbf{u} has broadly the same form as it would have in the absence of the ion phase, but of reduced magnitude. Limitation of the polar-cap area by the introduction of a dead zone, as in the following paragraph, also reduces the acceleration potential difference by a factor ζ which is shape-dependent but satisfies $1/4 < \zeta < 1/2$ for the semi-circular form assumed. Even so, we predict that ions from the central regions of the polar cap will often be too energetic to give the gain necessary for the non-linearity and plasma turbulence which are believed to be the source of the emission. Thus it is anticipated that, in many cases, the source of observable

emission will be confined to a band on the polar-cap surface close to the boundary \mathbf{u}_0 .

This is shown schematically in Fig. 1 which is a polar diagram showing the angular relations between the line of sight, spin $\mathbf{\Omega}$, and the tangents to the active open magnetosphere flux lines at altitude η . If \mathbf{u}_0 is here the boundary of the active polar-cap surface, the tangent at η is at an angle $\theta_0 = 3\eta^{1/2} \mathbf{u}_0 / 2R$ to the magnetic axis for a dipole field. The papers by Muslimov & Harding (2004, 2009) indicate that for general values of ψ , the inclination of the magnetic axis to $\mathbf{\Omega}$, the original Arons & Scharlemann (1979) division of the open magnetosphere into favourably and unfavourably-curved magnetic flux lines has some physical basis. For this reason we assume a semi-circular polar cap having a radius \mathbf{u}_0 given by equation (1). Also shown is the curve made by the transit of the open magnetosphere across the line of sight, for a particular case in which the latter is at a small angle with $\mathbf{\Omega}$. This is the $P = 0.645$ s PSR J0815+0939 (Champion et al 2005). The relation between the transit curve and open magnetosphere is drawn (approximately) to scale at an altitude $\eta = 10$, consistent with the work of Hassall et al (2012), so that the integrated profile has the observed width of 100° . The value of ψ is then $\sim 174^\circ$, and the number of components observed within the integrated pulse profile is equal to the number of times the line of sight crosses the emission band. It is seen immediately, in principle, how the four components of this pulsar arise and it is also possible to envisage other polar-cap shapes that would give four intersections per transit.

However, the specific case chosen here should not be considered too seriously because it appears to us that the real shape of the polar cap in cases where ψ is close to either 0 or 180° is particularly obscure. There appear to be no published papers that have considered such small inclinations. But for pulsars with more general values of ψ , the origin of two-component (referred to as single-cone) emission is obvious for almost any shape of polar cap. As an example, we refer to B1133+16 which has been observed over a wide range of frequencies by Hassall et al (2012). Reference to Fig. 1 shows that the outer and the central components can be easily understood. Thus the angular separation of the two outer components at 181 MHz, assuming emission at $\eta = 10$, should be $2\theta_0 \csc \psi = 8.6^\circ$ for the inclination $\psi = 180^\circ - 51^\circ = 129^\circ$ assumed by Hassall et al, to be compared with the observed value of 8.2° . The observed separation at the lowest frequency, 48 MHz, is rather larger (12.3°) but we do not regard this discrepancy as serious because this pulsar does exhibit some degree of radius-to-frequency mapping. Apart from these geometrical considerations, it is also easy to see how simple ion-phase motions give rise to the observed sub-pulse drift patterns, although a number of complicating factors exist.

Emission observed on the line of sight does not, in general, originate from a line on the polar-cap surface because the radiation decouples from the plasma over a finite interval of altitude. But there is an additional reason which is that, quite naturally for the class of mechanism we assume, the radiation emitted is not precisely parallel with the local magnetic flux density. Referring again to B1133+16, we note that the observed angular widths of the outer components are not inconsistent with those values of k_{\perp}/k_{\parallel} , where \mathbf{k} is the radiation wave-vector, which appear possible for

the quasi-longitudinal Langmuir mode introduced by Asseo, Pelletier & Sol (1990) and described in the present context by Jones (2012). Thus the ions producing radiation on the line of sight are actually emitted from the intersection of a finite band on the polar cap with the peripheral band shown in Fig. 1.

A further complication is that, for simplicity, the study of quasi-longitudinal Langmuir modes by Asseo et al (1990) from which equation (2) follows is essentially one-dimensional. But because we are concerned with emission from a peripheral band, as in Fig. 1, it is necessary to consider the lateral dimension of the emission region in relation to the observer-frame wavelength of the radiation. In general, there is a difference of one or two orders of magnitude. However, this may limit the extent to which ions from close to \mathbf{u}_0 with Lorentz factors near unity can be efficient emitters. But these considerations do not seriously affect the arguments which follow.

In relation to sub-pulse formation, the program described in Section 3 (see Jones 2013b) indicates the formation of clusters of ion-phase elements near the boundary \mathbf{u}_0 , but with no long-term stability. A system of organized ion-zone motion leading to sub-pulse formation and drift is shown by the arrows in the peripheral polar-cap band in Fig.1. We emphasize that organized motion over the whole polar cap is not needed and may not occur. The features of ion-zone motion that lead to this conclusion will be discussed in the following paragraph. Also, there is usually too little amplitude gain given by equation (2) for motion in the central region of the polar cap to be observed. We emphasize that long-term ion-zone stability is not needed as it would be in continuous carousel motion because an individual zone survives for only a single transit. Also the number of zones present at a given instant need not be an integer because one may be in a state of partial termination at \mathbf{u}_0 .

The way in which zones move was described in Section 5.1 of Jones (2013b), but is shown here in one dimension in Fig. 2, which assumes the idealized proton formation Green function mentioned in Section 2 and a value of the parameter $\tilde{K} = 3$. For either the ideal or the true Green function, motion or change of shape of any ion-zone boundary in two dimensions is determined solely by the following factors.

(i) Any element of area within an ion zone reverts to the proton phase when proton creation is sufficient to give a proton number density $n_p > 0$ at the top of its LTE ion atmosphere. For the model described in Sections 2 and 3, this occurs after a time τ_p .

(ii) Any element of area in a proton zone reverts to the ion phase when its proton number density falls to $n_p = 0$.

(iii) The speed and direction of motion of any element of ion-zone boundary is determined by the local value of $\nabla_{\mathbf{u}} n_p$. The rate of decrease of n_p at any point is constant, determined by the Goldreich-Julian current density. The direction of motion is then that of the least gradient.

Time-averaged values of \tilde{K} and hence of n_p are greatest in the central region of the polar cap and are lower near \mathbf{u}_0 . Clearly, movement within the peripheral band is strongly favoured. It is essentially one-dimensional and can be in either direction with a velocity v on the polar-cap surface given by $w = v\tau_p$, where w is the zone width. Proton zones then are of length $\tilde{K}w$. In a real system, the zeros in the surface proton number density at the leading and trailing

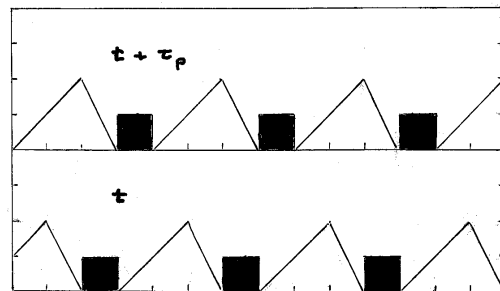


Figure 2. Ion-zone motion with velocity v is shown in one dimension for idealized proton diffusion, the horizontal axis being distance in units of $v\tau_p$. There are two vertical scales: the ion-zone current density (solid black) in units of $\rho_{GJ}c$, and for the line diagram giving the proton number density n_p in units of ρ_{GJ}/e . The maximum value of n_p is $\tilde{K} - 1$. The duration of the proton phase at any point is $\tilde{K}\tau_p$, with $\tilde{K} = 3$ in the diagram. An ion zone advances as the proton number density in front of it is depleted at a rate given by the Goldreich-Julian flux. The lower panel is at time t and the upper at $t + \tau_p$. The zeros in n_p remain for the true proton diffusion Green function, although the detailed shape of the n_p -distribution would change.

edges of an ion zone would remain, but for the correct Green function, both protons and ions are accelerated during the ion phase. We suggest that the velocity is defined by τ_p and by w , and that the magnitude of w is determined by Poisson's equation and by the photo-ionization and reverse-electron flow processes, that is, the tendency to cluster as found in the model. A further factor that might be relevant to the size of w is that electromagnetic showers also produce neutrons. The probability that a neutron would survive to reach the top of the LTE atmosphere is hard to estimate but (n, γ) reactions could mediate processes that are non-local, unlike those described in Section 2. However, organized motion need not be universal. Thus the possible states of the polar-cap are consistent with classes of coherent or diffuse drifting seen by Weltevrede et al.

Our model predicts that $P_3 = (\tilde{K} + 1)\tau_p$, and estimates of τ_p , and of \tilde{K} in the peripheral polar-cap band, give values of the order of 2 – 3 s (see Jones 2013b). Neither of the two parameters is other than a slowly-varying function of the basic pulsar parameters, P , B , $P/2\dot{P}$, and this is consistent with the conclusion of the Weltevrede et al survey. Measured values P_3 are largely within the 1 – 10 s interval, which is relatively compact for pulsar physics, but many authors have suggested that aliasing is present. Thus the distribution of true values of P_3 (or of the speed v on the polar cap) may be even more compact. Aliasing can be present in the results of periodic sampling of any system, including the model of this paper, and is a possible explanation for those few relatively large P_3 that are seen. But it is not required for bi-directional drifting.

The organized drift shown in Fig. 1 corresponds with the mirrored drift patterns observed in J0815+0939 and does so without the need for aliasing. (We note, however, that the behaviour of the first drift band seen by Champion et al is

indistinct. This could be a consequence of the direction of drift being almost perpendicular to the transit curve, which may also explain the longitude-stationary class of drift noted by Weltevrede et al.) Linear motions may result in the collision of two ion zones moving in opposite directions. The result of such a collision can be seen by imagining that the mirror image of Fig. 2 is placed adjacent to its right-hand side. The two zones touch after the proton zone separating them becomes exhausted and at a time τ_p later both terminate, having effectively annihilated leaving a proton zone. An ion zone simply terminates on impact with the polar-cap boundary.

The central region of the polar cap is the source of what is referred to as core emission. It may or may not be observable depending on the rate of growth given by equation (2). In many instances, the local value of $\gamma_{A,Z}$ will be too large for the necessary growth. The region has, in general, larger values of \bar{K} than in the peripheral band and behaviour that is less organized and more chaotic is anticipated.

5 CONCLUSIONS

The motivation for this work has been to construct a physical framework forming a basis for understanding how and why the many different observed phenomena occur. The mode changes, nulls, and sub-pulse drifts are to a large extent individual in character. It is true that there are distributions of rotation period, polar magnetic field, and of the inclinations of the line of sight and magnetic axis to Ω . But we regard it as questionable that Maxwell's equations with the appropriate boundary conditions and with the basic processes of quantum electrodynamics can provide an understanding of the complex phenomena that are seen in many specific pulsars.

A positive feature of the present model is that it does not require special values of the surface magnetic field. Whilst Geppert et al (2013) have demonstrated a field amplification of almost an order of magnitude for an initial dipole component of 10^{13} G, it is not clear from their paper whether amplification factors of $10^2 - 10^3$ would be possible to produce fields of about $\sim 10^{14}$ G in a large fraction of the pulsar population. Also, we do not believe that the photo-production of protons by the reverse electron flux in the $\mathbf{E} \neq 0$ polar cap has no observational consequences and so can be neglected.

The proton cohesive energy is negligible, even at 10^{14} G, and therefore an atmosphere would form if the production rate exceeded the Goldreich-Julian flux. Accelerated protons have a negligible pair-production rate, and there is no obvious mechanism for coherent curvature radiation. If high- B magnetic anomalies exist in some pulsars and are strong enough to produce the $\mathbf{E}_{\parallel} \neq 0$ condition at the polar cap, the proton-emission phase would interrupt this for substantial intervals of time so that their radio emission would be intermittent, possibly as in the Rotating Radio Transients (RRAT).

There is no obvious way in which the neutron-star surface can be involved in the case of $\Omega \cdot \mathbf{B} > 0$ pulsars because electrons are the only negatively-charged particles which can form a polar-cap current density. But the polar-cap alignment $\Omega \cdot \mathbf{B} < 0$ introduces two further variables both of

which, unfortunately, are not well known. These are the nuclear charge Z_s of surface ions and the polar-cap surface temperature T_s that is effective in photo-ionization of accelerated ions. It also introduces bi-stability in the composition of the accelerated ion beam.

Previous work (Jones 2013b) has demonstrated how this bi-stability distributed over the polar cap leads to potential fluctuations, on time-scales of the order of τ_p , and to the formation of localized areas from which the accelerated plasma has the properties necessary for rapid growth of a quasi-longitudinal Langmuir mode. These are the sub-pulses observed in pulsars with ages $\sim 1 - 10$ Myr, or more, and we propose that our model provides a sound physical basis for their formation. They do not have the long-term stability needed for a continuous circulation model, but we have pointed out in Section 4 that such motion is not needed and that a subpulse need survive only for the transit of no more than a polar-cap radius.

The physical processes which form the basis of the model are both prosaic and well-established. Provided neutron stars with $\Omega \cdot \mathbf{B} < 0$ exist, these processes must be present. They do not rely on high polar magnetic-flux densities except for the generation the modest acceleration potential differences which are needed. In general, there is no requirement that the basic parameters should have values within specified intervals and most neutron stars formed with this alignment should pass through an epoch of nulls, sub-pulse drift, and possibly mode-changes. The exception and the particular difficulty of the model is its dependence on the surface temperature T_s . This is the surface temperature of the area which is the source of the blackbody radiation effective in photo-ionization. It subtends, perhaps, a steradian centred on the polar cap and owing to anisotropy of the thermal conductivity, is likely to be at a higher temperature than the mean for the whole star. The model indicates that the important temperatures are those within a factor of approximately two of 4×10^5 K at the neutron-star surface, or 3×10^5 K as seen by a distant observer. These are very low, not observable for a compact object, but can be maintained by quite modest forms of dissipation. They must be attained during some interval in the life of the star, but it does not appear possible to estimate with confidence the length of that epoch.

The model is a physics-based framework but unfortunately the extent to which it is either capable of prediction or of being falsified is limited. In particular, sub-pulse movement is not easily predictable. We have attempted to show that organized motion can occur in a band at the polar-cap perimeter, and is responsible for the sub-pulse drift observed. But in general, the state of the entire polar cap is chaotic. However, given the heterogeneity of mode-changes, nulls, and sub-pulse drift, the search for a simple physical theory may well prove futile. The most direct evidence for ionic rather than electron-positron plasma appears to be from emission-altitude measurements in pulsars with favourable signal-to-noise ratios, such as those of Hassall et al (2012). Further measurements of this kind, should they prove possible, will be of considerable interest.

ACKNOWLEDGMENTS

The author thanks the referee for extensive comments that have greatly improved the presentation of this work.

REFERENCES

- Arons J., Scharlemann E. T., 1979, *ApJ*, 231, 854
Asseo E., Pelletier G., Sol H., 1990, *MNRAS*, 247, 529
Bhattacharyya B., Gupta Y., Gil J., Sendyk M., 2007, *MNRAS*, 377, L10
Bhattacharyya B., Gupta Y., Gil J., 2009, *MNRAS*, 398, 1435
Buschauer R., Benford B., 1977, *MNRAS*, 179, 99
Champion D. J., et al, 2005, *MNRAS*, 363, 929
Deshpande A. A., Rankin J. M., 1999, *ApJ*, 524, 1008
Deshpande A. A., Rankin J. M., 2001, *MNRAS*, 322, 438
Geppert U., Gil J., Melikidze G., 2013, *MNRAS*, 435, 3262
Gil J., Melikidze G. I., Geppert U., 2003, *A&A*, 407, 315
Gupta Y., Gil J., Kijak J., Sendyk M., 2004, *A&A*, 426, 229
Harding A. K., Muslimov A. G., 2001, *ApJ*, 556, 987
Hassall T. E. et al, 2012, *A&A*, 543, A66
Honnappa S., Lewandowski W., Kijak J., Deshpande A. A., Gil J., Maron O., Jessner A., 2012, *MNRAS*, 421, 1996
Janssen G. H., van Leeuwen J., 2004, *A&A*, 425, 255
Jones P. B., 1985, *Phys. Rev. Lett.*, 55, 1338
Jones P. B., 2012, *MNRAS*, 423, 3502
Jones P. B., 2013a, *MNRAS*, 435, L11
Jones P. B., 2013b, *MNRAS*, 431, 2756
Leeuwen J. van, Timokhin A. N., 2012, *ApJ*, 752, 155
Medin Z., Lai D., 2006, *Phys. Rev. A.*, 74, 062508
Mitra D., Rankin J. M., 2008, *MNRAS*, 385, 606
Muslimov A. G., Harding A. K., 2004, *ApJ*, 617, 471
Muslimov A. G., Harding A. K., 2009, *ApJ*, 692, 140
Muslimov A. G., Tsygan A. I., 1992, *MNRAS*, 255, 61
Rankin J. M., Wright G. A. E., Brown A. M., 2013, *MNRAS*, 433, 445
Rankin J. M., Wright G. A. E., 2008, *MNRAS*, 385, 1923
Ruderman M. A., Sutherland P. G., 1975, *ApJ*, 196, 51
Weltevrede P., Edwards R. T., Stappers B. W., 2006, *A&A*, 445, 243

This paper has been typeset from a \TeX / \LaTeX file prepared by the author.